Chinese Physics Letters

LETTER

# Superconductivity with Macroscopic Time-Reversal Symmetry Breaking in the Presence of Loop-Current Fluctuations

Cite as: Zenghui Fan *et al*. 2026 *Chin. Phys. Lett.* **43** 080702

DOI CSTR

## Recommended Articles

**Parameter-Dependent Superconducting Transition Temperature in a Sign-Problem-Free Bilayer Model**
Runyu Ma, Zenghui Fan, Tianxing Ma, and Congjun Wu
*Chin. Phys. Lett.* **42**, 110705 (2025)

**Observation of Zero-Energy Modes with Possible Time-Reversal Symmetry Breaking on Step Edge of $CaKFe_4As_4$**
Lu Cao *et al*.
*Chin. Phys. Lett.* **41**, 117401 (2024)

**Loop-Current Fluctuations Mediated Chiral *d*-Wave Pairing in Kagome Lattice**
Qi-Fang Li, Gaopei Pan, Xu Zhang, Satoru Nakatsuji, Weilun Jiang, Xiao Yan Xu, and Xianxin Wu
*Chin. Phys. Lett.* **42**, 057302 (2025)

**Layer-Valley Hall Effect under Inversion and Time-Reversal Symmetries**
Jiaojiao Zhao, Gui-Bin Liu, Peng Chen, Yugui Yao, Guangyu Zhang, and Luojun Du
*Chin. Phys. Lett.* **41**, (2024)

**Symmetry Breaking Dynamics in Quantum Many-Body Systems**
Hui Yu, Zi-Xiang Li, and Shi-Xin Zhang
*Chin. Phys. Lett.* **42**, 110602 (2025)

**Universal Behavior in Entanglement Entropy Reveals Quantum Criticality and Underlying Symmetry Breaking**
Zhe Wang, Zehui Deng, Zenan Liu, Zhiyan Wang, Yi-Ming Ding, Long Zhang, Wenan Guo, and Zheng Yan
*Chin. Phys. Lett.* **42**, 110712 (2025)

A series journal of Chinese Physical Society distributed by IOP Publishing

Chinese Physics Letters

*Chin. Phys. Lett.* **43** 080702 (2026)

LETTER

DOI: 10.1088/0256-307X/43/8/080702
CSTR: 32039.14.0256-307X.43.8.080702

# Superconductivity with Macroscopic Time-Reversal Symmetry Breaking in the Presence of Loop-Current Fluctuations

**Zenghui Fan[1], Runyu Ma[1], Stefano Chesi[2], Congjun Wu[3,4,5,6,*], and Tianxing Ma[1,*]**

[1]School of Physics and Astronomy, Beijing Normal University, and Key Laboratory of Multiscale Spin Physics (Beijing Normal University), Ministry of Education, Beijing 100875, China
[2]Beijing Computational Science Research Center, Beijing 100084, China
[3]New Cornerstone Science Laboratory, Department of Physics, School of Science, Westlake University, Hangzhou 310024, China
[4]Institute for Theoretical Sciences, Westlake University, Hangzhou 310024, China
[5]Key Laboratory for Quantum Materials of Zhejiang Province, School of Science, Westlake University, Hangzhou 310024, China
[6]Institute of Natural Sciences, Westlake Institute for Advanced Study, Hangzhou 310024, China

[*]Corresponding authors. Email: wucongjun@westlake.edu.cn; txma@bnu.edu.cn

**Loop currents (LCs) have been proposed in various superconductors and recently confirmed in kagome materials, raising a fundamental question regarding their intrinsic connection to superconductivity (SC). Here, we investigate this issue using a sign-problem-free bilayer *t*-$J_\perp$-*V* model that hosts a spontaneous interlayer loop-current (ILC) parent state, via unbiased projector quantum Monte Carlo simulations. Near half-filling, interlayer interactions stabilize ILC order that breaks time-reversal symmetry (TRS). Upon hole doping, the ILC order is suppressed, while interlayer *s*-wave SC emerges with optimal doping behavior. Specifically, superconducting correlations are enhanced in the regime where ILC order is weakened, demonstrating an intimate interplay between the two phases. The resulting phase diagram reveals a transition from the half-filled ILC parent state to doped SC, reminiscent of the evolution from antiferromagnetic order to SC in cuprates, except that LCs involve orbital magnetism. Strikingly, a significant coexistence region emerges near the quantum critical regime, where SC develops with the persistence of residual ILC correlations and appreciable fluctuations, giving rise to a SC state with macroscopic TRS breaking. Our results establish a minimal theoretical framework for exploring the connection between LCs and SC, and reveal a promising route to TRS breaking in superconductors, offering important insights into the unconventional SC in LC systems.**

## Introduction

The discovery of copper-based superconductors [1] established high-temperature superconductivity (SC) as a central topic in condensed matter physics. Clarifying its mechanism is essential for discovering new high-$T_c$ materials. In many kinds of superconductors [1−4], SC emerges alongside various fluctuations, which are often closely associated with its formation [5−7]. For instance, in doped cuprates, antiferromagnetic (AFM) fluctuations have been closely tied to spin-singlet pairing near a quantum critical point (QCP) [8,9]. Other fluctuations, including charge density waves [10], spin density waves [11], and stripe order [12], also play important roles, resulting in rich phase diagrams. Recently, significant attention has been drawn to orbital magnetic fluctuations that break time-reversal symmetry (TRS) in kagome superconductors [13−20]. This orbital magnetism is associated with a pattern of spontaneously flowing currents. According to a theory by Bloch [21−23], such currents must form closed loops, known as loop currents (LCs), to avoid forbidden global currents. Yet, the intrinsic connection between LC fluctuations and SC remains a fundamental open question.

In strongly correlated systems, magnetic fluctuations arise not only from spin-related interactions but also in the orbital sector through LCs. The identification of such currents in diverse superconducting systems—including cuprates [24−26], bilayer graphene [27], and kagome systems [13−20]—has made their relationship with SC a critical and actively debated issue.

In high-$T_c$ cuprates, LC order has been proposed as a hidden order underlying the pseudogap phase [24−26]. Its possible connection to $d_{x^2-y^2}$-wave superconducting pairing near the quantum critical point has been extensively discussed [28]. Furthermore, LC order has been invoked to interpret polarized neutron scattering experiments [29−32]. However, the absence of LC signatures in other studies [33−36] has led to persistent controversy regarding the interplay between LC fluctuations and SC. Recently, the observation of a TRS-breaking charge density wave in kagome superconductors $AV_3Sb_5$ ($A$ = K, Rb, Cs) [13−18] has revitalized the LC proposal and intensified interest in their relationship with SC [37−42]. Theoretical models attribute these currents to nonlocal interactions [41−43], yet an unbiased, numerically exact characterization of the LC-SC interplay remains elusive due to the fermion sign problem. One promising strategy to circumvent this challenge is the interlayer loop-current (ILC) framework. In prior work by one of the authors [44], this configuration was termed interlayer staggered currents, providing a foundation for our present study.

To address this challenge, we introduce a minimal bilayer model in which spontaneous ILCs emerge from unbiased interlayer exchange and Coulomb repulsive interactions, free from the fermion sign problem. LC models typically involve directly incorporating a biased weighting of the LC pattern into the Hamiltonian. By contrast, our framework avoids such presumptions, allowing an intrinsic ILC parent to develop microscopically. The resulting bilayer structure and significant interlayer exchange coupling are shared features with a broader class of correlated electron systems, including the recently discovered bilayer nickelate $La_3Ni_2O_7$ [4,45,46], where the coexistence of SC and TRS breaking has recently been discovered [47]. However, we must explicitly acknowledge that realistic nickelates and other materials always host the complex multi-orbital electronic structures and interactions beyond the scope of our model. Therefore, our primary aim is not to quantitatively describe a specific material, but to

Received 9 May 2026; accepted 29 June 2026; published 22 July 2026
© 2026 Chinese Physical Society and IOP Publishing Ltd. All rights, including for text and data mining, AI training, and similar technologies, are reserved.

Check for updates

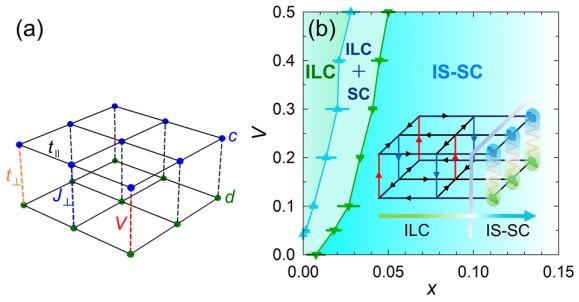


**Fig. 1.** (a) Sketch of the bilayer model with intralayer nearest-neighbor hopping $t_\parallel$, interlayer on-site hopping $t_\perp$, interlayer antiferromagnetic spin-exchange coupling $J_\perp$, and interlayer Coulomb repulsion $V$. (b) Phase diagram as a function of hole doping $x$ and interlayer Coulomb repulsion $V$ at $J_\perp = 2$, showing the interlayer loop-current phase (ILC), the interlayer $s$-wave superconducting phase (IS-SC), and their coexistence phase (ILC+SC) featured by the superconductivity with macroscopic time-reversal symmetry breaking. The green and blue solid lines mark the phase boundaries of ILC and IS-SC, respectively, as determined by finite-size scaling. Inset: schematic illustrations of the ILC and IS-SC patterns.

establish a controlled theoretical platform for investigating the interplay between LCs and SC in layered correlated systems.

In this work, we investigate a $t$-$J_\perp$-$V$ model on a hole-doped bilayer square lattice, as sketched in Fig. 1(a), using the unbiased projector quantum Monte Carlo (PQMC) method [48,49]. This model is free from the sign problem due to Kramers invariance [50], thereby overcoming the difficulties of simulating doped systems and yielding numerically exact results. Our calculations demonstrate that spontaneous ILCs are stabilized by nearest-neighbor interlayer interactions near half-filling, forming an ILC parent state. Upon hole doping, the ILC order is rapidly suppressed, while an interlayer $s$-wave SC (IS-SC) emerges with an optimal doping behavior, reminiscent of the evolution from an AFM parent to SC, except that LCs involve orbital rather than spin magnetism. Structure factors and correlation lengths reveal an intimate interplay between ILC correlations and IS-SC, with superconducting correlations strengthening in the regime where the ILC order is suppressed. The resulting phase diagram, summarized in Fig. 1(b), highlights a transition from the ILC state to SC, with a coexistence phase emerging near the quantum critical regime. This coexistence is characterized by a SC state with macroscopic TRS breaking, reflecting the persistence of LC correlations and appreciable fluctuations in proximity to the phase boundary. Our model clearly uncovers an intimate connection between LCs and SC, demonstrating that the SC with macroscopic TRS breaking develops in the significant critical regime where LC fluctuations remain appreciable.

## Model and Methods

The $t$-$J_\perp$-$V$ Hamiltonian studied in this work is defined as

$$\begin{aligned} H = & -t_\parallel \sum_{\langle ij\rangle\sigma} (c^\dagger_{i\sigma} c_{j\sigma} + d^\dagger_{i\sigma} d_{j\sigma} + \text{H.c.}) \\ & -t_\perp \sum_{i\sigma} (c^\dagger_{i\sigma} d_{i\sigma} + \text{H.c.}) - \mu \sum_{i\sigma} (c^\dagger_{i\sigma} c_{i\sigma} + d^\dagger_{i\sigma} d_{i\sigma}) \\ & + J_\perp \sum_i \boldsymbol{S}_{i,c} \cdot \boldsymbol{S}_{i,d} + V \sum_i (n_{i,c} - 1)(n_{i,d} - 1), \end{aligned} \tag{1}$$

where $c_{i\sigma}$ ($c^\dagger_{i\sigma}$) and $d_{i\sigma}$ ($d^\dagger_{i\sigma}$) are electron annihilation (creation) operators with spin $\sigma = \uparrow, \downarrow$ at site $\boldsymbol{i}$ for the upper and lower layers, respectively. The spin operator is $\boldsymbol{S}_{i,c} = c^\dagger_i \boldsymbol{\sigma} c_i$, where $c_i = (c_{i\uparrow}, c_{i\downarrow})^{\mathrm{T}}$ is a two-component spinor and $\boldsymbol{\sigma}$ denotes the vector of Pauli matrices. The occupation number operator is $n_{i,c} = c^\dagger_i c_i = \sum_\sigma c^\dagger_{i\sigma} c_{i\sigma}$. The noninteracting part of Eq. (1) includes the intralayer nearest-neighbor hopping $t_\parallel$, the interlayer on-site hopping $t_\perp$, and the chemical potential $\mu$. The interaction terms describe interlayer on-site couplings, consisting of the Heisenberg spin-exchange interaction $J_\perp$ and the Coulomb repulsion $V$.

The absence of the sign problem in this model originates from Kramers invariance associated with a spin-3/2 fermionic representation within the SO(5) algebra [50], which is equivalent to the spin-1/2 bilayer formulation [44,51–53]. Exploiting this property, the Hamiltonian can be recast as

$$\begin{aligned} H = & -t_\parallel \sum_{\langle ij\rangle} (\psi^\dagger_i \psi_j + \text{H.c.}) - t_\perp \sum_i \psi^\dagger_i \Gamma^5 \psi_i \\ & -\mu \sum_i \psi^\dagger_i \psi_i - \sum_i \left\{ \frac{g_1}{2} \sum_{a=1,5} \left( \frac{1}{2} \psi^\dagger_i \Gamma^a \psi_i \right)^2 \right. \\ & \left. + \frac{g_2}{2} \left[ \sum_{a=2,3,4} \left( \frac{1}{2} \psi^\dagger_i \Gamma^a \psi_i \right)^2 + 3(\psi^\dagger_i \psi_i - 2)^2 \right] \right\}, \end{aligned} \tag{2}$$

with $\psi_i = \left[ c_{i\uparrow}, c_{i\downarrow}, d_{i\uparrow}, d_{i\downarrow} \right]^{\mathrm{T}}$ and the five $\Gamma$ matrices [50]

$$\Gamma^1 = \begin{pmatrix} 0 & -iI \\ iI & 0 \end{pmatrix}; \quad \Gamma^{2,3,4} = \begin{pmatrix} \boldsymbol{\sigma} & 0 \\ 0 & -\boldsymbol{\sigma} \end{pmatrix}; \quad \Gamma^5 = \begin{pmatrix} 0 & I \\ I & 0 \end{pmatrix}, \tag{3}$$

where $I$ denotes the $2\times 2$ identity matrix and $\boldsymbol{\sigma}$ the vector of Pauli matrices. The Kramers transformation is defined as $\mathcal{T} = \Gamma^1 \Gamma^3 C$, where $C$ means complex conjugate. $\mathcal{T}$ is an antiunitary time-reversal operation accompanied by swapping the upper and lower layers with $\mathcal{T}^2 = -1$, which ensures

$$\mathcal{T} I \mathcal{T}^{-1} = I; \quad \mathcal{T} \Gamma^a \mathcal{T}^{-1} = \Gamma^a. \tag{4}$$

Therefore, the Hamiltonian (2) is Kramers invariant, and it is equivalent to Eq. (1) with $g_1 = V/4 + 3J_\perp/16$ and $g_2 = -V/4 + J_\perp/16$.

We employ the PQMC method to obtain the ground-state wave function $|\Psi_{\mathrm{g}}\rangle$ by projecting a nondegenerate trial state $|\Psi_{\mathrm{t}}\rangle$ ($\langle \Psi_{\mathrm{t}} | \Psi_{\mathrm{g}} \rangle \neq 0$) via the projection operator $\exp(-\theta H/2)$ [48]. In general, the Hubbard–Stratonovich transformation used to decouple interaction terms may introduce negative fermion determinants, leading to the sign problem. In the present model, Kramers invariance ensures that eigenvalues of the fermion matrix appear in complex-conjugate pairs [53], guaranteeing a positive-definite determinant when $g_1, g_2 \geq 0$, i.e., $-3J_\perp/4 \leq V \leq J_\perp/4$. Throughout this work, we set $t_\parallel = 1$ as the energy unit, and fix $J_\perp = 2$ and $t_\perp = 0.1$ to realize a sizable interlayer AFM exchange. We then focus on the effects of the interlayer Coulomb interaction $V$ and hole doping $x$.

To characterize the ILCs, we employ the structure factor of the interlayer currents:

$$O_{\mathrm{ic}}(\boldsymbol{q}) = \frac{1}{N} \sum_{i,j} \exp(\mathrm{i}\boldsymbol{q} \cdot (\boldsymbol{i} - \boldsymbol{j})) \langle O^{\mathrm{ic}}_i O^{\mathrm{ic}}_j \rangle, \tag{5}$$

where $N$ is the number of unit cells, and the interlayer current operator is defined as

$$O^{\mathrm{ic}}_i = \frac{\mathrm{i}}{2} \sum_\sigma (c^\dagger_{i\sigma} d_{i\sigma} - d^\dagger_{i\sigma} c_{i\sigma}). \tag{6}$$

The ILCs exhibit a staggered pattern of interlayer currents accompanied by alternating intralayer currents, as illustrated in the inset of Fig. 1(b). In this work, we adopt the staggered interlayer current component as the representative descriptor of the global ILC order, as it provides the leading contribution. Accordingly, the ILC order is characterized by the structure factor at wavevector $(\pi,\pi)$, defined as $O_{\mathrm{ILC}} \equiv O_{\mathrm{ic}}(\pi,\pi)$. We have also verified the intralayer current pattern (see Section S1 of the Supplemental Material (SM) for further details). It is worth noting that an interlayer bond order, which can be induced by $J_\perp$ [54], is degenerate with the interlayer current order in the absence of $t_\perp$, but is suppressed once $t_\perp$ is introduced, becoming subdominant to the current order. Therefore, we do not consider the bond order in this work (see Section S2 of the SM for details).

Physically, the Kramers time-reversal symmetry of sign-problem-free models always tends to introduce a Cooper-like instability, leading to SC [55,56]. We therefore investigate the SC in our bilayer system. We define the IS-SC pairing structure factor as

$$O_{\rm sc}(\boldsymbol{q}) = \frac{1}{N}\sum_{i,j}\exp(\mathrm{i}\boldsymbol{q}\cdot(\boldsymbol{i}-\boldsymbol{j}))\langle\Delta_s^{\dagger}(\boldsymbol{i})\Delta_s(\boldsymbol{j})\rangle, \tag{7}$$

where the interlayer s-wave pairing operator is defined as

$$\Delta_s^{\dagger}(\boldsymbol{i}) = \frac{1}{\sqrt{2}}\left(c_{i\uparrow}d_{i\downarrow} - c_{i\downarrow}d_{i\uparrow}\right)^{\dagger}. \tag{8}$$

The uniform component $O_{\rm sc}(0,0)$ is taken as the measure of IS-SC order, denoted by $O_{\rm IS-SC}$. We also confirm that interlayer pairing is dominant among the SC channels in this system (see Section S4 of the SM).

To further characterize the interplay between different orders, we compute the correlation length at fixed system size $L$, defined as

$$\xi(L) = \frac{1}{2\sin(\pi/L)}\left(\frac{O_\alpha(\boldsymbol{Q})}{O_\alpha(\boldsymbol{Q}+\delta\boldsymbol{q})} - 1\right)^{1/2}, \tag{9}$$

where $\boldsymbol{Q}$ denotes the ordering wavevector associated with each order parameter, and $\delta\boldsymbol{q} = (2\pi/L, 0)$ is the minimal momentum shift [57]. The quantity $\xi(L)$ provides a measure of the spatial extent of correlations and is useful for analyzing the competition and proximity between different orders.

## Results and Discussion

LCs are thought to bear an important connection to SC, as highlighted by proposals in high-$T_c$ cuprates [28,58]. Recent discussions of interlayer $s$-wave pairing in bilayer systems have emphasized the role of strong interlayer exchange coupling [46]. Motivated by these considerations, our bilayer model enables a controlled investigation of the interplay between LCs and SC. The resulting phase diagram [Fig. 1(b)] reveals a transition from a TRS-breaking ILC parent state to a superconducting phase. Near half-filling, spontaneous ILCs are stabilized by interlayer exchange $J_\perp = 2$ and further enhanced by interlayer Coulomb repulsion $V$, thereby extending the ILC regime. With increasing hole doping, the ILC order is suppressed, while IS-SC emerges, which leads to the ILC-SC transition. This behavior indicates a close interplay between the suppression of LC order and the emergence of SC. The overall evolution is reminiscent of the transition from an AFM parent to SC in cuprates, with the distinction that LCs involve orbital rather than spin magnetism.

In our model, ILCs intrinsically break TRS, and the ground-state phase diagram reveals a significant coexistence region of ILC and IS-SC phases near the phase boundary, demonstrating the persistence of residual LC order within SC. In this regime, SC emerges and develops alongside residual LC correlations and appreciable fluctuations, naturally leading to SC in the macroscopic TRS-breaking background. Notably, this TRS breaking is not intrinsically established in SC pairing channels, but merely results in a SC state with macroscopic TRS breaking (see Section S5 of the SM for details). Even within the predominantly superconducting region near the ILC phase, signatures of TRS breaking may persist due to the presence of residual LC fluctuations. This significant coexistence region offers an important perspective for understanding how macroscopic TRS breaking can manifest within the SC state in layered correlated systems.

We first examine the structure factors of the interlayer current and the interlayer $s$-wave pairing [Eqs. (5) and (7)]. The interlayer pairing and current structure factors peak at wavevectors $(0,0)$ and $(\pi,\pi)$, respectively. The latter indicates a staggered ILC with broken TRS in our sign-problem-free model (see Section S1 of the SM for detailed evidence). Figure 2 displays the ILC and IS-SC structure factors as functions of doping $x$ for different interlayer Coulomb repulsions $V$ at a fixed system size $L = 12$. The ILC structure factor decreases rapidly with doping but is significantly enhanced by $V$ near half-filling. In contrast, the IS-SC structure factor is suppressed by $V$ and enhanced by doping, exhibiting an optimal doping behavior. Strikingly, the enhancement of the IS-SC structure factor below the optimal doping level occurs in the regime where the ILC correlations are significantly suppressed. This correspondence indicates a close interplay between the suppression of ILC correlations and the emergence of SC. The opposing effects of $V$ can be understood as follows: $V$ breaks the charge occupation balance between the two layers, thereby enhancing interlayer charge transfer while suppressing uniform interlayer charge pairing. Analogously, we also consider the AFM structure factor, which is likewise suppressed by $V$ (see Section S3 of the SM for details). The role of $V$ is analogous to the nonlocal interaction proposed for LCs in kagome models [41,42]. Overall, these results indicate an intriguing competition between ILC order and IS-SC in the bilayer system, with SC developing in proximity to the suppression of ILC correlations.

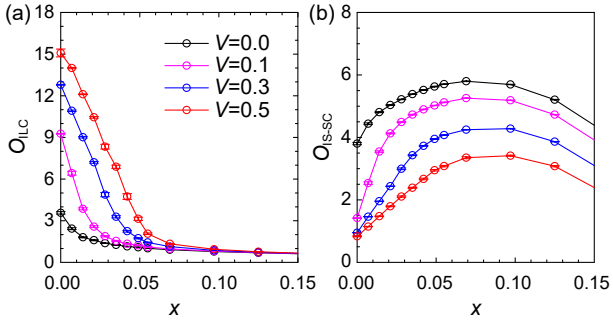


**Fig. 2.** Structure factors (a) $O_{\rm ILC}$ and (b) $O_{\rm IS\text{-}SC}$ as functions of hole doping $x$ for different interlayer Coulomb repulsions $V$. The ILC structure factor is suppressed by $x$ and significantly enhanced by $V$ near half-filling, while the IS-SC structure factor is suppressed by $V$ and exhibits optimal doping behavior.

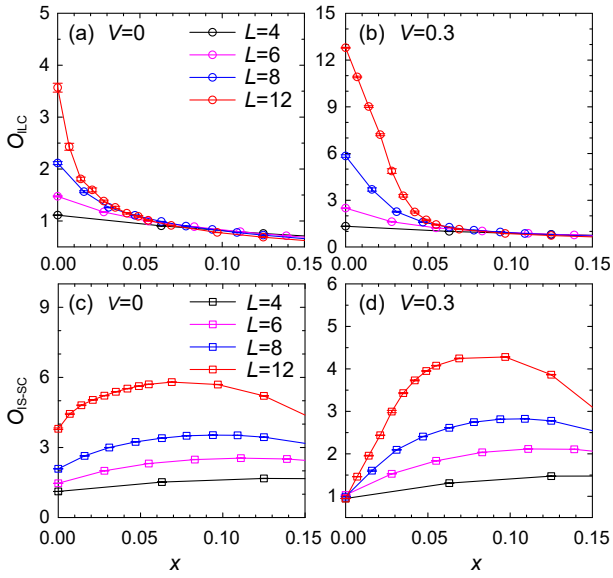


**Fig. 3.** Structure factors $O_{\rm ILC}$ and $O_{\rm IS\text{-}SC}$ as functions of doping $x$ with different lattice size $L$ at (a) $V = 0$ and (b) $V = 0.3$ for ILC, and at (c) $V = 0$ and (d) $V = 0.3$ for IS-SC. The $L$-dependence of structure factor is revealed in this figure, where the growth with increasing $L$ indicates the trend for ordering, while the saturation indicates disorder.

To assess the presence of long-range order, we examine the system-size $L$ dependence of the structure factors, which qualitatively reflects the behavior of the correlation length $\xi$, as shown in Fig. 3. In a disordered regime (i.e., $\xi \ll L$), the structure factor becomes nearly independent of $L$ and saturates to a value proportional to $\xi^2$. Conversely, in an ordered regime (i.e., $\xi \gg L$), it is limited by the system size and increases with $L$. For the ILC structure factor in Figs. 3(a) and 3(b), the $L$ dependence is suppressed by doping $x$ but enhanced by the interlayer repulsion $V$ near half-filling. In contrast, the IS-SC structure factor exhibits pronounced $L$ dependence over a broad

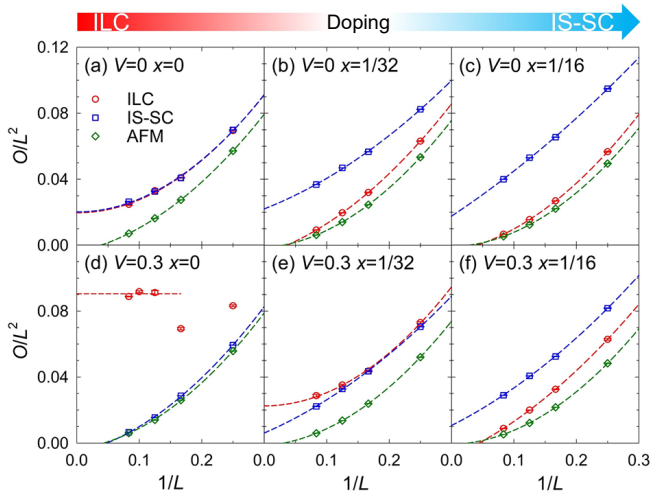


**Fig. 4.** Structure factors $O/L^2$ as functions of the reciprocal of lattice size $1/L$ for ILC, IS-SC and AFM. The data with different sizes are extrapolated to the thermodynamic limit at different doping $x = 0$, $x = 1/32$, and $x = 1/16$ for the interlayer repulsion (a)–(c) $V = 0$ and (d)–(f) $V = 0.3$, respectively. The finite-size scaling is performed by the polynomial fittings to the data of $L = 4, 6, 8, 12$ denoted by dashed lines. An additional $L = 10$ data set for ILC is included at (d) and the red flat dashed line of (d) is a guide to the eye.

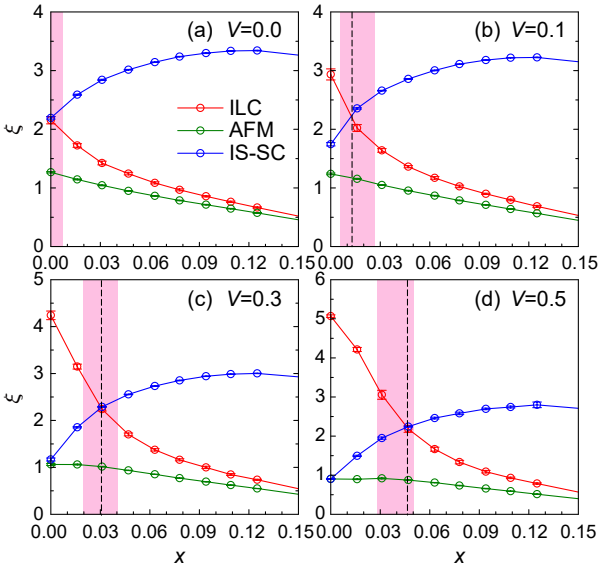


**Fig. 5.** Correlation lengths $\xi$ as functions of doping $x$ for ILC, AFM, and IS-SC with different interlayer repulsion (a) $V = 0.0$, (b) $V = 0.1$, (c) $V = 0.3$, and (d) $V = 0.5$ at $L = 8$. The crossover where the dominant order changes is marked by a black dashed line. These crossovers consistently fall into the pink areas which record the region of coexistence phase as shown in Fig. 1.

doping range [Figs. 3(c) and 3(d)], which is reduced by $V$ especially near half-filling [e.g., for $V = 0.3$ in panel (d)]. Notably, as doping increases to the optimal level, the $L$ dependence of the IS-SC develops to a maximum while the $L$ dependence of ILC is simultaneously suppressed but remains finite. This behavior underscores the persistence of residual LC correlations and appreciable fluctuations in the emergence and development of SC near the quantum critical regime.

To further determine the phase boundaries, we perform a finite-size scaling analysis of the structure factors to extract their values in the thermodynamic limit, as shown in Fig. 4, based on the scaling hypothesis $O_\alpha(L)/L^2 = a\xi^2/L^2 + b/L + c$ [59]. We first consider the case with no interlayer repulsion, $V = 0$, as shown in Figs. 4(a)–4(c). At half-filling ($x = 0$), we find that ILC establishes long-range order in the thermodynamic limit, as indicated by a finite intercept at $L \to \infty$. This demonstrates the qualitative role of interlayer exchange $J_\perp$ in stabilizing ILCs in the absence of $V$. Additionally, IS-SC similarly exhibits long-range order, indicating a coexistence phase at this parameter set. With increased doping to $x = 1/32$ and $x = 1/16$, the IS-SC long-range order persists, while the ILC order is suppressed. Introducing a finite interlayer repulsion $V = 0.3$ alters this picture, as shown in Figs. 4(d)–4(f). At half-filling, the ILC order is strongly enhanced and robust, while IS-SC order is absent. Particularly, in panel (d), the upward curvature of the $O_{\mathrm{ILC}}/L^2$ data at $L = 6$ strongly indicates a pronounced tendency toward ILC ordering. To ensure reliability, the inclusion of $L = 10$ data in panel (d) confirms this trend, showing a large $O_{\mathrm{ILC}}/L^2$ approaching saturation at large $L$. At $x = 1/32$, both ILC and IS-SC exhibit long-range order, but by $x = 1/16$, the ILC order vanishes, leaving only the IS-SC long-range order. These results clearly display a transition from a half-filled ILC parent to a doped IS-SC phase, resembling the conventional AFM-SC transition. Strikingly, the concomitant long-range orders for ILC and IS-SC at different $V$ and $x$ indicate a significant parameter-dependent coexistence phase near the quantum critical point, as shown in Fig. 1(b), where the persistence of residual LC order and its appreciable fluctuations give rise to the SC with macroscopic TRS breaking. We also note that AFM order is absent for all parameters in our system, as shown in all panels of Fig. 4. An interpolation method was used to obtain data at fixed dopings for different system sizes. The phase boundaries for ILC and IS-SC are determined from this detailed finite-size scaling and summarized in the phase diagram of Fig. 1(b).

The correlation length $\xi$ defined in Eq. (9) provides a direct measure of the spatial extent of correlations and the competition among different orders, as illustrated in Fig. 5. Across all parameters, the AFM correlation length remains smaller than those of ILC and IS-SC, consistent with the finite-size scaling analysis presented above. A key observation is the contrasting evolution of the ILC and IS-SC correlation lengths upon doping: the ILC correlation length decreases while the IS-SC correlation length increases, indicating strong competition between these two phases. The crossover of these curves in Fig. 5 marks the boundary between regimes dominated by different correlations. As $V$ increases, this critical doping shifts to higher values, and the crossover consistently occurs within the narrow coexistence region of the phase diagram, highlighted in pink in Fig. 5. Significantly, the evolutions for both ILC and IS-SC correlation lengths are continuous at a similar rate, and consequently the crossover point shares a moderate and commensurate level of correlation length for ILC and IS-SC, demonstrating the persistence of residual ILC correlations near the phase boundary where associated LC fluctuations are appreciable. The results further support that the SC state with macroscopic TRS breaking develops in the significant critical regime where LC fluctuations remain appreciable. Furthermore, the correlation length analysis also confirms the dominance of interlayer s-wave pairing in the SC channel for our bilayer model (see Section S4 of the SM).

## Conclusions

Centering on the recently revitalized topic of LCs, we directly address a fundamental question of their connection to SC through a minimal quantum model hosting a spontaneous LC parent state. Employing unbiased PQMC simulations, we study a microscopic $t$-$J_\perp$-$V$ model with three key features: (1) spontaneous generation of ILCs near half-filling without imposing explicit bias, leading to TRS breaking; (2) absence of the fermion sign problem due to Kramers invariance, enabling numerically exact simulations for doped systems; and (3) a bilayer structure with significant interlayer exchange coupling, capturing generic ingredients of layered correlated electron systems.

Our results show that ILCs are stabilized by interlayer exchange $J_\perp$ and further enhanced by interlayer repulsion $V$ near half-filling, forming an intrinsic ILC parent state. Upon hole doping, the ILC order is suppressed, while IS-SC develops with an optimal doping profile. Intriguingly, the superconducting correlations strengthen in the

regime where ILC order is weakened as doping increases to the optimal level, indicating a close competition between the two phases. Based on the analysis of long-range order, we construct a phase diagram [Fig. 1(b)] that is consistent with a transition from the half-filled ILC parent to a doped IS-SC phase. This evolution is reminiscent of the AFM-SC transition in cuprates, except that LCs involve orbital rather than spin magnetism. Importantly, a coexistence region emerges near the quantum critical region, demonstrating the persistence of residual LC correlations and appreciable fluctuations within SC. In this significant region, the presence of LC order and its associated fluctuations gives rise to a SC state with macroscopic TRS breaking.

In summary, our results highlight a pivotal topic regarding the connection between LCs and SC in a controlled, sign-problem-free setting. The present study demonstrates a promising route to TRS breaking in superconductors arising from the persistence of LC correlations and associated fluctuations. More broadly, our work provides a minimal theoretical framework for exploring the interplay between LCs and SC, offering important insights into related phenomena in layered correlated systems and unconventional SC in LC systems.

Our study may also connect to experimental advances in ultracold atom systems. Mixed-dimensional bilayer optical lattices with strong interlayer spin-exchange interactions have recently been realized [60,61]. Furthermore, related $t$-$J$ models with rung Coulomb repulsion have been proposed for implementation in ultracold atom platforms [62,63]. These developments highlight ultracold atom systems as promising platforms for realizing our minimal model and exploring the connection between LC correlations and SC in a controlled setting.

## Conflict of Interest

The authors declare that they have no conflict of interest.

## Author Contributions

Z. Fan performed the simulations, analyzed the figures, and wrote the paper. R. Ma and S. Chesi participated in discussion and writing. C. Wu provided academic guidance. T. Ma directed the investigation and writing of the paper. The manuscript reflects the contributions of all authors.

## Acknowledgements

This work was supported by the National Natural Science Foundation of China (Grant Nos. 12474218, 12234016, and 12574274), the Beijing Natural Science Foundation (Nos. 1242022 and 1252022), and the New Cornerstone Science Foundation. The numerical simulations in this work were performed at the HSCC of Beijing Normal University.

## References

[1] Bednorz J G and Muller K A 1986 *Z. Physik B - Condensed Matter* **64** 189
[2] Kamihara Y, Watanabe T, Hirano M, and Hosono H 2008 *J. Am. Chem. Soc.* **130** 3296
[3] Jerome D, Mazaud A, Ribault M, and Bechgaard K 1980 *J. Physique Lett.* **41** 95
[4] Sun H, Huo M, Hu X, Li J, Liu Z, Han Y, Tang L, Mao Z, Yang P, Wang B, Cheng J, Yao D X, Zhang G M, and Wang M 2023 *Nature* **621** 493
[5] Nakatsuji S, Kuga K, Machida Y, Tayama T, Sakakibara T, Karaki Y, Ishimoto H, Yonezawa S, Maeno Y, Pearson E, Lonzarich G G, Balicas L, Lee H, and Fisk Z 2008 *Nat. Phys.* **4** 603
[6] Matsubayashi K, Tanaka T, Sakai A, Nakatsuji S, Kubo Y, and Uwatoko Y 2012 *Phys. Rev. Lett.* **109** 187004
[7] Sakai A, Matsumoto Y, Fu M, Isomae T, Tsujimoto M, O'Farrell E, Nishio-Hamane D, and Nakatsuji S 2025 *Nat. Commun.* **16** 2114
[8] Keimer B, Kivelson S A, Norman M R, Uchida S, and Zaanen J 2015 *Nature* **518** 179
[9] Yuan J, Chen Q, Jiang K *et al* 2022 *Nature* **602** 431
[10] Li L J, O'Farrell E C T, Loh K P, Eda G, Ozyilmaz B, and Neto A H C 2016 *Nature* **529** 185
[11] Zhao D, Zhou Y, Huo M, Wang Y, Nie L, Yang Y, Ying J, Wang M, Wu T, and Chen X 2025 *Sci. Bull.* **70** 1239
[12] Zheng B X, Chung C M, Corboz P, Ehlers G, Qin M P, Noack R M, Shi H, White S R, Zhang S, and Chan G K L 2017 *Science* **358** 1155
[13] Mielke C, Das D, Yin J X, Liu H, Gupta R, Jiang Y X, Medarde M, Wu X, Lei H C, Chang J, Dai P, Si Q, Miao H, Thomale R, Neupert T, Shi Y, Khasanov R, Hasan M Z, Luetkens H, and Guguchia Z 2022 *Nature* **602** 245
[14] Guo C, Putzke C, Konyzheva S, Huang X, Gutierrez-Amigo M, Errea I, Chen D, Vergniory M G, Felser C, Fischer M H, Neupert T, and Moll P J W 2022 *Nature* **611** 461
[15] Xing Y, Bae S, Ritz E *et al*. 2024 *Nature* **631** 60
[16] Asaba T, Onishi A, Kageyama Y *et al*. 2024 *Nat. Phys.* **20** 40
[17] Feng X, Jiang K, Wang Z, and Hu J 2021 *Sci. Bull.* **66** 1384
[18] Liu H, Duan S, Liu X, Liu Z, Wang S, Gu L, Huang J, Yang W, Liu J, Qian D, Guo Y, and Zhang W 2025 *Sci. Bull.* **70** 1211
[19] Elmers H J, Tkach O, Lytvynenko Y *et al*. 2025 *Phys. Rev. Lett.* **134** 096401
[20] Ma H Y, Yin J X, Zahid Hasan M, and Liu J 2024 *Chin. Phys. Lett.* **41** 047103
[21] Bohm D 1949 *Phys. Rev.* **75** 502
[22] Ohashi Y and Momoi T 1996 *J. Phys. Soc. Jpn.* **65** 3254
[23] Watanabe H 2022 *Phys. Rev. Res.* **4** 013043
[24] Varma C M 1997 *Phys. Rev. B* **55** 14554
[25] Simon M E and Varma C M 2003 *Phys. Rev. B* **67** 054511
[26] Varma C M 2006 *Phys. Rev. B* **73** 155113
[27] Zhu L, Aji V, and Varma C M 2013 *Phys. Rev. B* **87** 035427
[28] Aji V, Shekhter A, and Varma C M 2010 *Phys. Rev. B* **81** 064515
[29] Fauqué B, Sidis Y, Hinkov V, Pailhès S, Lin C T, Chaud X, and Bourges P 2006 *Phys. Rev. Lett.* **96** 197001
[30] Li Y, Balédent V, Barišić N, Cho Y, Fauqué B, Sidis Y, Yu G, Zhao X, Bourges P, and Greven M 2008 *Nature* **455** 372
[31] Li Y, Balédent V, Yu G *et al*. 2010 *Nature* **468** 283
[32] Bourges P, Bounoua D, and Sidis Y 2021 *Cr. Phys.* **22** 1
[33] Mounce A M, Oh S, Lee J A, Halperin W P, Reyes A P, Kuhns P L, Chan M K, Dorow C, Ji L, Xia D, Zhao X, and Greven M 2013 *Phys. Rev. Lett.* **111** 187003
[34] Wu T, Mayaffre H, Krämer S, Horvatić M, Berthier C, Hardy W N, Liang R, Bonn D A, and Julien M H 2015 *Nat. Commun.* **6** 6438
[35] Gheidi S, Akintola K, Fang A C Y, Sundar S, Côté A M, Dunsiger S R, Gu G D, and Sonier J E 2020 *Phys. Rev. B* **101** 184511
[36] Zhu Z H, Zhang J, Ding Z F *et al*. 2021 *Phys. Rev. B* **103** 134426
[37] Palle G, Ojajärvi R, Fernandes R M, and Schmalian J 2024 *Sci. Adv.* **10** eadn3662
[38] Cui C, Zhao J Y, and Weng Z Y 2026 arXiv: 2602.21206 [cond-mat.str-el]
[39] Wang X Q, Luo G Q, Liu J Y, Huang G H, Li Z X, Wu C, Hemmerich A, and Xu Z F 2023 *Phys. Rev. Lett.* **131** 226001
[40] Li Q F, Pan G, Zhang X, Nakatsuji S, Jiang W, Xu X Y, and Wu X 2025 *Chin. Phys. Lett.* **42** 057302
[41] Fu R, Zhan J, Dürrnagel M, Hohmann H, Thomale R, Hu J, Wang Z, Zhou S, and Wu X 2025 *Nat. Sci. Rev.* **12** nwaf414
[42] Zhan J, Hohmann H, Dürrnagel M, Fu R, Zhou S, Wang Z, Thomale R, Wu X, and Hu J 2026 *Phys. Rev. Lett.* **136** 126001
[43] Lin Y H, Dong J W, Fu R, Wu X, Wang Z, and Zhou S 2025 *Chin. Phys. Lett.* **42** 080709
[44] Capponi S, Wu C, and Zhang S C 2004 *Phys. Rev. B* **70** 220505
[45] Xie T, Huo M, Ni X, Shen F, Huang X, Sun H, Walker H C, Adroja D, Yu D, Shen B, He L, Cao K, and Wang M 2024 *Sci. Bull.* **69** 3221
[46] Lu C, Pan Z, Yang F, and Wu C 2024 *Phys. Rev. Lett.* **132** 146002
[47] Ji H, Xie Z, Chen Y, Zhou G, Pan L, Wang H, Huang H, Ge J, Liu Y, Zhang G M, Wang Z, Xue Q K, Chen Z, and Wang J 2026 arXiv: 2508.16412 [cond-mat.supr-con]
[48] Assaad F F and Evertz H G 2008 *Computational Many-Particle Physics* p. 277

[49] Li Z X, Wang F, Yao H, and Lee D H 2016 *Sci. Bull.* **61** 925
[50] Wu C, Hu J P, and Zhang S C 2003 *Phys. Rev. Lett.* **91** 186402
[51] Ma T, Wang D, and Wu C 2022 *Phys. Rev. B* **106** 054510
[52] Ma R and Ma T 2023 *Phys. Rev. B* **107** 214509
[53] Wu C and Zhang S C 2005 *Phys. Rev. B* **71** 155115
[54] Bejas M, Wu X, Chakraborty D, Schnyder A P, and Greco A 2025 *Phys. Rev. B* **111** 144514
[55] Grossman O and Berg E 2023 *Phys. Rev. Lett.* **131** 056501
[56] Zhang X and Bultinck N 2025 *Phys. Rev. B* **112** 125110
[57] Campostrini M, Pelissetto A, and Vicari E 2014 *Phys. Rev. B* **89** 094516
[58] Weber C, Läuchli A, Mila F, and Giamarchi T 2009 *Phys. Rev. Lett.* **102** 017005
[59] Assaad F F and Herbut I F 2013 *Phys. Rev. X* **3** 031010
[60] Hirthe S, Chalopin T, Bourgund D, Bojovic P, Bohrdt A, Demler E, Grusdt F, Bloch I, and Hilker T A 2023 *Nature* **613** 463
[61] Bohrdt A, Homeier L, Bloch I, Demler E, and Grusdt F 2022 *Nat. Phys.* **18** 651
[62] Lange H, Homeier L, Demler E, Schollwöck U, Grusdt F, and Bohrdt A 2024 *Phys. Rev. B* **109** 045127
[63] Lange H, Homeier L, Demler E, Schollwöck U, Bohrdt A, and Grusdt F 2024 *Phys. Rev. B* **110** L081113